Inorg. Chem. **2007**, *46*, 3395–3406

Inorganic Chemistry
Article

Self-Assembly Reactions between the Cis-Protected Metal Corners (N–N)M^{II} (N–N = Ethylenediamine, 4,4′-Substituted 2,2′-Bipyridine; M = Pd, Pt) and the Fluorinated Edge 1,4-Bis(4-pyridyl)tetrafluorobenzene

Montserrat Ferrer,*,† Albert Gutiérrez,† Mounia Mounir,† Oriol Rossell,† Eliseo Ruiz,†
Alexander Rang,‡ and Marianne Engeser‡

Departament de Química Inorgànica, Universitat de Barcelona, c/Martí i Franquès 1-11, 08028
Barcelona, Spain, and Kekulé-Institut für Organische Chemie und Biochemie der Universität,
Gerhard-Domagk-Strassse 1, D-53121 Bonn, Germany

Received December 12, 2006

The self-assembly reactions between the fluorinated ditopic ligand 1,4-bis(4-pyridyl)tetrafluorobenzene (**A**) and different nitrogen-protected palladium(II) and platinum(II) complexes have been investigated. While dynamic equilibria between molecular triangles and squares were observed when the diimine compounds 4,4′-R_2bipy (bipy = 2,2′-bipyridine; R = H, Me, *t*-Bu) were employed as ancillary ligands, only square species were obtained from ethylenediamine (en) derivatives. Characterization of the obtained metallomacrocycles was accomplished by ^{1}H and ^{19}F NMR spectroscopy in combination with electrospray ionization Fourier transform ion cyclotron resonance mass spectrometry (ESI-FT-ICR). Molecular dynamics simulations (UFF) have been performed to interpret the influence of the fluorinated ring on the square/triangle relative stability. Density functional calculations using the GIAO method have been employed for the interpretation of the chemical shift assignments. The study of the ability of these compounds to act as hosts of electron-rich aromatic guests has shown that the palladium ethylenediamine square is capable of establishing this type of intermolecular interaction exclusively in aqueous media. The host–guest stoichiometry and association constants have been determined by ^{1}H NMR spectroscopy.

Introduction

The design and preparation through self-assembly of discrete molecular architectures using polytopic organic ligands and transition metal complexes has undergone significant development for more than one decade.[1−10] There are numerous examples of metal-mediated self-assembly architectures including dimers,[11−13] triangles,[14−22] squares,[8,23−30] rectangles,[10,31−36] pentagons,[37,38] hexagons,[39,40] and many

---

* To whom correspondence should be addressed. E-mail: montse.ferrer@qi.ub.es.
† Universitat de Barcelona.
‡ Kekulé-Institut für Organische Chemie und Biochemie der Universität.

(1) Jones, C. J. *Chem. Soc. Rev.* **1998**, *27*, 289−299.
(2) Fujita, M. *Chem. Soc. Rev.* **1998**, *27*, 417−425.
(3) Swiegers, G. F.; Malefetse, T. J. *Chem. Rev.* **2000**, *100*, 3483−3537.
(4) Leininger, S.; Olenyuk, B.; Stang, P. J. *Chem. Rev.* **2000**, *100*, 853−907.
(5) Holliday, B. J.; Mirkin, C. A. *Angew. Chem., Int. Ed.* **2001**, *40*, 2022−2043.
(6) Swiegers, G. F.; Malefetse, T. J. *Coord. Chem. Rev.* **2002**, *225*, 91−121.
(7) Schalley, C. A.; Lutzen, A.; Albrecht, M. *Chem.—Eur. J.* **2004**, *10*, 1072−1080.
(8) Wurthner, F.; You, C. C.; Saha-Moller, C. R. *Chem. Soc. Rev.* **2004**, *33*, 133−146.
(9) Fujita, M.; Tominaga, M.; Hori, A.; Therrien, B. *Acc. Chem. Res.* **2005**, *38*, 369−378.
(10) Thanasekaran, P.; Liao, R. T.; Liu, Y. H.; Rajendran, T.; Rajagopal, S.; Lu, K. L. *Coord. Chem. Rev.* **2005**, *249*, 1085−1110.
(11) Lee, S. J.; Kim, J. S.; Lin, W. *Inorg. Chem.* **2004**, *43*, 6579−6588.
(12) Shen, W. Z.; Gupta, D.; Lippert, B. *Inorg. Chem.* **2005**, *44*, 8249−8258.
(13) Beves, J. E.; Chapman, B. E.; Kuchel, P. W.; Lindoy, L. F.; McMurtrie, J.; McPartlin, M.; Thordarson, P.; Wei, G. *Dalton. Trans.* **2006**, 744−750.
(14) Clegg, J. K.; Lindoy, L. F.; Moubaraki, B.; Murray, K. S.; McMurtrie, J. C. *Dalton. Trans.* **2004**, 2417−2423.
(15) Qin, Z. Q.; Jennings, M. C.; Puddephatt, R. J. *Inorg. Chem.* **2002**, *41*, 3967−3974.
(16) Qin, Z. Q.; Jennings, M. C.; Puddephatt, R. J. *Inorg. Chem.* **2003**, *42*, 1956−1965.
(17) Mimassi, L.; Guyard-Duhayon, C.; Rager, M. N.; Amouri, H. *Inorg. Chem.* **2004**, *43*, 6644−6649.
(18) Fornies, J.; Gomez, J.; Lalinde, E.; Moreno, M. T. *Chem.*—Eur. J. **2004**, *10*, 888−898.
(19) Galindo, M. A.; Navarro, J. A. R.; Romero, M. A.; Quiros, M. *Dalton. Trans.* **2004**, 1563−1566.
(20) Martin-Redondo, M. P.; Ludmila Scoles, L.; Sterenberg, B. T.; Udachin, K. A.; Carty, A. J. *J. Am. Chem. Soc.* **2005**, *127*, 5038−5039.
(21) Hwang, S. H.; Moorefield, C. N.; Fronczek, F. R.; Lukoyanova, O.; Echegoyen, L.; Newkome, G. R. *Chem. Commun.* **2005**, 713−715.

10.1021/ic062373s CCC: $37.00

other more complex topologies.[38,41−46] In many cases, the information stored in the building blocks, i.e., the number of receptor and acceptor groups and their relative disposition in space, allows one to predict the structure of the resulting product. However, when there is no thermodynamic preference for one species, or when effects like steric strain or electrostatic repulsion are taken into account, two or more species may coexist in dynamic equilibrium in solution.

In particular, the combination of cis-protected, square planar Pd^{II} and Pt^{II} complexes with linear ligands has been observed to yield, in some cases, interesting equilibria between molecular triangles and logically expected squares.[8,47−52] Detailed studies[47−52] revealed that the triangle/square ratio depends upon several factors, such as the environmental conditions (concentration, temperature, and/or pressure) and/or the characteristics of the building blocks. More specifically, the nature of the ancillary ligand on the metal corners seems to play a decisive role. Thus, for example, since Fujita reported the first self-assembled square[53] supramolecule incorporating (en)Pd^{II} at the corners, the combination of this unit and its analogous (en)Pt^{II} with a series of ditopic nonchelating ligands has led to the formation in solution of a series of squares[9,54,55] that, in most cases, have been reported to be in equilibrium with their triangular counterparts.[47,48,50] By contrast, when the ancillary ethylenediamine ligand on the Pd^{II} or Pt^{II} centers was replaced by the more rigid 2,2′-bipyridine either triangular species[15,16] or square/triangle mixtures[28,50,56] were obtained instead.

We recently reported[51,52] our findings on the self-assembly reaction between a series of *cis*-diphosphine Pd^{II} and Pt^{II} complexes and the rigid fluorinated ligand 1,4-bis(4-pyridyl)-tetrafluorobenzene. Although we designed the latter ligand with the aim of generating electron-poor cavities capable of encapsulating electron-rich aromatic compounds, we have not found any evidence of such a phenomenon with any of the synthesized diphosphine macrocycles.

With this in mind, we decided to extend our studies with the fluorinated organic edge **A** by exploring its solution self-assembly reactions with the nitrogen-blocked Pd^{II} and Pt^{II} diamine (en)M^{II} (M = Pd, Pt) and diimine (4,4′-R_2bipy)M^{II} (R = H, Me, *t*-Bu) metallic units. The use of N-donors as bipyridine or ethylenediamine instead of diphosphine ligands not only provided both electronic and sterical changes but also allowed us to obtain a series of water-soluble macrocycles, suitable for analyzing the contributions of hydrophobic and/or electrostatic effects in the encapsulation of electron-rich aromatic guests.

An integrated approach, involving electrospray ionization Fourier transform ion cyclotron resonance (ESI-FT-ICR) mass spectrometry, computational studies, and NMR investigations in solution, has been used to characterize the resulting structures.

Experimental Section

All manipulations were performed under prepurified N_2 using standard Schlenk techniques. All solvents were distilled from appropriate drying agents. Commercial reagents 4-bromopyridine hydrochloride, 1,4-dibromotetrafluorobenzene, 2,2′-bipy, 4,4′-Me_2-2,2′-bipy, 4,4′-*t*-Bu_2-2,2′-bipy, and ethylenediamine were used as received. The compounds [$PdCl_2$(COD)],[57] [$PdCl_2$(4,4′-Me_2bipy)],[58]

---

(22) Cotton, F. A.; Liu, C. Y.; Murillo, C. A.; Wang, X. P. *Inorg. Chem.* **2006**, *45*, 2619−2626.

(23) Bera, J. K.; Bacsa, J.; Smucker, B. W.; Dunbar, K. R. *Eur. J. Inorg. Chem.* **2004**, 368−375.

(24) Kraft, S.; Hanuschek, E.; Beckhaus, R.; Haase, D.; Saak, W. *Chem.*—Eur. J. **2005**, *11*, 969−978.

(25) Song, L. C.; Jin, G. X.; Wang, H. T.; Zhang, W. X.; Hu, Q. M. *Organometallics* **2005**, *24*, 6464−6471.

(26) Karadas, F.; Schelter, E. J.; Prosvirin, A. V.; Bacsa, J.; Dunbar, K. R. *Chem. Commun.* **2005**, 1414−1416.

(27) Sautter, A.; Kaletas, B. K.; Schmid, D. G.; Dobrawa, R.; Zimine, M.; Jung, G.; van Stokkum, I. H. M.; De Cola, L.; Williams, R. M.; Wurthner, F. *J. Am. Chem. Soc.* **2005**, *127*, 6719−6729.

(28) Zhang, L.; Niu, Y. H.; Jen, A. K.-Y.; Lin, W. *Chem. Commun.* **2005**, 1002−1004.

(29) Jude, H.; Disteldorf, H.; Fischer, S.; Wedge, T.; Hawkridge, A. M.; Arif, A. M.; Hawthorne, M. F.; Muddiman, D. C.; Stang, P. J. *J. Am. Chem. Soc.* **2005**, *127*, 12131−12139.

(30) Cotton, F. A.; Murillo, C. A.; Yu, R. M. *Dalton. Trans.* **2006**, 3900−3905.

(31) Mukherjee, P. S.; Min, K. S.; Arif, A. M.; Stang, P. J. *Inorg. Chem.* **2004**, *43*, 6345−6350.

(32) Dinolfo, P. H.; Hupp, J. T. *J. Am. Chem. Soc.* **2004**, *126*, 16814−16819.

(33) Han, W. S.; Lee, S. W. *Dalton. Trans.* **2004**, 1656−1663.

(34) Lin, R.; Yip, J. H. K.; Zhang, K.; Koh, L. L.; Wong, K. Y.; Ho, K. P. *J. Am. Chem. Soc.* **2004**, *126*, 15852−15869.

(35) Addicott, C.; Oesterling, I.; Yamamoto, T.; Mullen, K.; Stang, P. J. *J. Org. Chem.* **2005**, *70*, 797−801.

(36) Toma, L. M.; Lescouezec, R.; Cangussu, D.; Llusar, R.; Mata, J.; Spey, S.; Thomas, J. A.; Lloret, F.; Julve, M. *Inorg. Chem. Commun.* **2005**, *8*, 382−385.

(37) Radhakrishnan, U.; Stang, P. J. *J. Org. Chem.* **2003**, *68*, 9209−9213.

(38) Jiang, H.; Lin, W. B. *J. Am. Chem. Soc.* **2006**, *128*, 11286−11297.

(39) Yamamoto, T.; Arif, A. M.; Stang, P. J. *J. Am. Chem. Soc.* **2003**, *125*, 12309−12317.

(40) Halper, S. R.; Cohen, S. M. *Angew. Chem., Int. Ed.* **2004**, *43*, 2385−2388.

(41) Reger, D. L.; Semeniuc, R. F.; Smith, M. D. *Inorg. Chem.* **2003**, *42*, 8137−8139.

(42) Kumazawa, K.; Yamanoi, Y.; Yoshizawa, M.; Kusukawa, T.; Fujita, M. *Angew. Chem., Int. Ed.* **2004**, *43*, 5936−5940.

(43) Kobayashi, K.; Yamada, Y.; Yamanaka, M.; Sei, Y.; Yamaguchi, K. *J. Am. Chem. Soc.* **2004**, *126*, 13896−13897.

(44) Paul, R. L.; Argent, S. P.; Jeffery, J. C.; Harding, L. P.; Lynam, J. M.; Ward, M. D. *Dalton. Trans.* **2004**, 3453−3458.

(45) Pinalli, R.; Cristini, V.; Sottili, V.; Geremia, S.; Campagnolo, M.; Caneschi, A.; Dalcanale, E. *J. Am. Chem. Soc.* **2004**, *126*, 6516−6517.

(46) Yoshizawa, M.; Nakagawa, N.; Kumazawa, K.; Nagao, M.; Kawano, M.; Ozeki, T.; Fujita, M. *Angew. Chem., Int. Ed.* **2005**, *44*, 1810−1813.

(47) Lee, S. B.; Hwang, S. G.; Chung, D. S.; Yun, H. S.; Hong, J. I. *Tetrahedron Lett.* **1998**, *39*, 873−876.

(48) Park, K. M.; Kim, S. Y.; Heo, J.; Whang, D.; Sakamoto, S.; Yamaguchi, K.; Kim, K. *J. Am. Chem. Soc.* **2002**, *124*, 2140−2147.

(49) Schweiger, M.; Seidel, S. R.; Arif, A. M.; Stang, P. J. *Inorg. Chem.* **2002**, *41*, 2556−2559.

(50) Fujita, M.; Sasaki, O.; Mitsuhashi, T.; Fujita, T.; Yazaki, J.; Yamaguchi, K.; Ogura, K. *Chem. Commun.* **1996**, 1535−1536.

(51) Ferrer, M.; Mounir, M.; Rossell, O.; Ruiz, E.; Maestro, M. A. *Inorg. Chem.* **2003**, *42*, 5890−5899.

(52) Ferrer, M.; Rodriguez, L.; Rossell, O. *J. Organomet. Chem.* **2003**, *681*, 158−166.

(53) Fujita, M.; Yazaki, J.; Ogura, K. *J. Am. Chem. Soc.* **1990**, *112*, 5645−5647.

(54) Orita, A.; Jiang, L. S.; Nakano, T.; Ma, N. C.; Otera, J. *Chem. Commun.* **2002**, 1362−1363.

(55) Yoshizawa, M.; Nagao, M.; Kumazawa, K.; Fujita, M. *J. Organomet. Chem.* **2005**, *690*, 5383−5388.

(56) Yu, S. Y.; Huang, H. P.; Li, S. H.; Jiao, Q.; Li, Y. Z.; Wu, B.; Sei, Y.; Yamaguchi, K.; Pan, Y. J.; Ma, H. W. *Inorg. Chem.* **2005**, *44*, 9471−9488.

(57) Drew, D.; Doyle, J. R. *Inorg. Syn.* **1990**, *28*, 346−349.

[$PtCl_2$(4,4′-Me_2bipy)],[59] [$Pd(NO_3)_2$(bipy)] (**1a**),[60] [$Pt(NO_3)_2$(bipy)] (**1b**),[61,62] [$Pd(NO_3)_2$(en)] (**4a**),[63] [$Pt(NO_3)_2$(en)] (**4b**),[64] [$Pd(OTf)_2$(bipy)] (**1c**),[65] [$Pt(OTf)_2$(bipy)] (**1d**),[66] [$Pd(OTf)_2$(4,4′-*t*-Bu_2bipy)] (**3a**),[15] [$Pt(OTf)_2$(4,4′-*t*-Bu_2bipy)] (**3b**),[67] and 1,4-bis(4-pyridyl)-tetrafluorobenzene (**A**)[51,68] were prepared as described previously.

Physical Measurements. Infrared spectra were recorded on a FT-IR 520 Nicolet spectrophotometer. ^1H NMR (δ(TMS) = 0.0 ppm) and ^{19}F NMR ($\delta(CFCl_3)$ = 0.0 ppm) spectra were performed on Bruker 500 DMX, Bruker DXR 250, Varian Inova 500, and Varian Unity 400 spectrometers at 25 °C unless otherwise stated. A ledbpgs2s (2D sequence with bipolar gradients for diffusion using stimulated echo and LED) was used for the diffusion experiment.[69] Elemental analyses of C, H, N, and S were carried out at the Serveis Científico-Tècnics of the Universitat de Barcelona.

ESI mass spectra were recorded on a Bruker APEX IV Fourier-transform ion cyclotron resonance (FT-ICR) mass spectrometer with a 7.05 T magnet and an Apollo electrospray (ESI) ion source equipped with an off-axis 70° spray needle. Typically, nitromethane solutions of the squares (100−200 μM) were used. Analyte solutions were introduced into the ion source with a syringe pump (Cole-Parmer Instruments, Series 74900) at flow rates of 3−4 μL/min. Ion transfer into the first of three differential pump stages in the ion source occurred through a glass capillary with a 0.5 mm inner diameter and nickel coatings at both ends. Ionization parameters were adjusted as follows: capillary voltage, −4.5 kV; end plate voltage, −4.0 kV; capexit voltage, 40−120 V; skimmer voltages, 5 V; temperature of drying gas, 40 °C. Nitrogen was used as nebulizing (25 psi) and drying gas (5 psi). The ions were accumulated in the instruments hexapole for 0.1−1 s, introduced into the FT-ICR cell, which was operated at pressures below 10^{-10} mbar, and detected by a standard excitation and detection sequence. For each measurement, 16−64 scans were averaged to improve the signal-to-noise ratio.

Job Plots. Equimolar solutions (2 mM) of **(4aA)$_4$** and the guests **II** and **III** (D_2O, 25 °C) were prepared and mixed in various ratios. ^1H NMR spectra of the solutions were recorded, and the changes in chemical shifts for the methyl protons of **II** and **III** were analyzed.

NMR Titrations. Stock solutions of the host (10 mM) and the guest (2 mM) were prepared in D_2O. A 500 μL portion of the guest solution was transferred to a NMR tube, and an initial spectrum was taken to determine the initial chemical shift of free guest. Aliquots of the host solution (10 μL initially and then 20−30 μL) were added to the guest solution. A ^1H NMR spectrum was recorded after each addition until no changes in the chemical shifts of the methyl protons of the guest were observed.

Computational Details. The calculation of the shielding shifts was carried out using the GIAO (gauge invariant atomic orbital) method[70] implemented in the Gaussian03 code.[71] The calculations were performed using the hybrid B3LYP functional.[72−74] We have employed Stoll−Preuss pseudopotentials for the platinum atoms[75] and a 6-31G* basis set[76] for the main group elements geometry in the geometry optimization. The IGLO-II basis set[70] was employed for the main group elements in the calculations of chemical shifts. Despite the presence of heavy metals, the use of the relativistic pseudopotentials provides good estimates of the shielding shifts of the neighbor atoms as it has been shown by Kaupp et al.[77,78]

[$Pd(OTf)_2$(4,4′-Me_2bipy)] (2c). A 106 mg amount (0.42 mmol) of solid AgOTf was added to a CH_2Cl_2 (25 mL) solution of 50 mg (0.14 mmol) of [$PdCl_2$(4,4′-Me_2bipy)]. The reaction mixture was stirred for 12 h with exclusion of light. After filtration, the resulting solution was concentrated to 10 mL in vacuum and a yellowish solid was precipitated upon addition of 20 mL of pentane. Subsequent recrystallization (CH_2Cl_2/pentane) gave 33 mg (40%) of pure **2c**. Anal. Calcd for $C_{14}H_{12}F_6N_2O_6PdS_2$: C, 28.56; H, 2.05; N, 4.75. Found: C, 28.74; H, 2.15; N, 4.80. ^1H NMR (250.1 MHz, CD_3NO_2): 8.14 (s, 2H, H_3, $H_{3'}$, Me_2bipy), 8.06 (d, J = 5.9 Hz, 2H, H_6, $H_{6'}$, Me_2bipy), 7.61 (d, J = 6 Hz, 2H, H_5, $H_{5'}$, Me_2bipy), 2.67 (s, 6H, CH_3, Me_2bipy). ν_{max}(KBr)/cm^{-1}: 1622, 829, 514 (Me_2bipy), 1250, 1172, 1031 (OTf).

[$Pt(OTf)_2$(4,4′-Me_2bipy)] (2d). A 100 mg amount (0.22 mmol) of [$PtCl_2$(4,4′-Me_2bipy)] was added to a 1.2 mL of CF_3SO_3H at room temperature. The reaction mixture was stirred for 24 h. After addition of 5 mL of Et_2O, a yellow solid was obtained that was filtered off, washed several times with Et_2O to eliminate the remaining acid, and dried in vacuum. Yield: 120 mg (80%). Anal. Calcd for $C_{14}H_{12}F_6N_2O_6PtS_2$: C, 24.82; H, 1.79; N, 4.14. Found: C, 24.74; H, 1.74; N, 4.27. ^1H NMR (250.1 MHz, CD_3NO_2): 8.47 (d, J = 6.2 Hz, 2H, H_6, $H_{6'}$, Me_2bipy), 8.21 (s, 2H, H_3, $H_{3'}$, Me_2bipy), 7.08 (d, J = 5.7 Hz, 2H, H_5, $H_{5'}$, Me_2bipy), 2.68 (s, 6H, CH_3, Me_2bipy). ν_{max}(KBr)/cm^{-1}: 1630, 827, 516 (Me_2bipy), 1250, 1174, 1031 (OTf).

Square/Triangle (1aA)$_4$/(1aA)$_3$. Solid 1,4-bis(4-pyridyl)tetrafluorobenzene (**A**) (20 mg, 0.06 mmol) was added to a CH_2Cl_2 (5 mL) suspension of [$Pd(NO_3)_2$(bipy)] (**1a**) (25 mg, 0.06 mmol) at room temperature. After 2 h of stirring, a yellowish solid precipitated. Filtration and drying in vacuum gave 37 mg (85%) of the product. **(1aA)$_4$**: ^1H NMR (500.1 MHz, D_2O) 9.21 (d, J = 7 Hz, 16H, $H_{\alpha-py}$), 8.37 (d, J = 8 Hz, 8H, H_3, $H_{3'}$, bipy), 8.27 (m, 8H, H_4, $H_{4'}$, bipy), 7.92 (d, J = 6.5 Hz, 16H, $H_{\beta-py}$), 7.49 (m, 8H, H_5, $H_{5'}$, bipy), 7.39 (d, J = 5.5 Hz, 8H, H_6, $H_{6'}$, bipy); ^{19}F NMR (376.5 MHz, D_2O) −142.90 (s, F_A). **(1aA)$_3$**: ^1H NMR (500.1 MHz,

---

(58) This compound was prepared in 85% yield, by mixing equimolar quantities of dichloro(1,5-cyclooctadiene)palladium(II) and 4,4′-dimethyl-2,2′-bypiridine in dichloromethane at room temperature. After 2 h of stirring, the formed orange solid was filtered off, washed with diethyl ether, and dried in vacuum.

(59) Yang, L.; Wimmer, F. L.; Wimmer, S.; Zhao, J. X.; Braterman, P. S. *J. Organomet. Chem.* **1996**, *525*, 1−8.

(60) Yu, S. Y.; Fujita, M.; Yamaguchi, K. *J. Chem. Soc., Dalton Trans.* **2001**, 3415−3416.

(61) Navarro, J. A. R.; Romero, M. A.; Salas, J. M.; Quiros, M. *Inorg. Chem.* **1997**, *36*, 3277−3283.

(62) Morgan, G. T.; Burstall, F. H. *J. Chem. Soc.* **1934**, 965−971.

(63) Fujita, M.; Aoyagi, M.; Ogura, K. *Inorg. Chim. Acta* **1996**, *246*, 53−57.

(64) Rochon, F. D.; Morneau, A. *Magn. Reson. Chem.* **1991**, *29*, 120−126.

(65) Diver, C.; Lawrance, G. A. *J. Chem. Soc., Dalton Trans.* **1988**, 931−934.

(66) Field, J. S.; Haines, R. J.; Summerton, G. C. *J. Coord. Chem.* **2003**, *56*, 1149−1155.

(67) Hill, G. S.; Rendina, L. M.; Puddephatt, R. J. *J. Chem. Soc., Dalton Trans.* **1996**, 1809−1813.

(68) Ferrer, M.; Gutierrez, A.; Mounir, M.; Solans, X.; Font-Bardia, M. *Acta Crystallogr., Sect. E* **2006**, *62*, o3213−o3214.

(69) Wu, D. H.; Chen, A. D.; Johnson, C. S. *J. Magn. Reson., Ser. A* **1995**, *115*, 260−264.

(70) Hehre, W.; Radom, L.; Schleyer, P. R. V.; Pople, J. A. *Ab Initio Molecular Orbital Theory*; Wiley: New York, 1986.

(71) *Gaussian 98 (Revision A.11)*; Gaussian, Inc.: Pittsburgh, PA, 1998.

(72) Becke, A. D. *J. Chem. Phys.* **1993**, *98*, 5648−5652.

(73) Becke, A. D. *Phys. Rev. A* **1988**, *38*, 3098.

(74) Lee, C. T.; Yang, W. T.; Parr, R. G. *Phys. Rev. B* **1988**, *37*, 785−789.

(75) Andrae, D.; Haussermann, U.; Dolg, M.; Stoll, H.; Preuss, H. *Theor. Chim. Acta* **1990**, *77*, 123−141.

(76) Kutzelnigg, W.; Fleischer, U.; Schindler, M. *NMR Basic Principles and Progress*; Springer-Verlag: New York, 1990.

(77) Kaupp, M.; Malkin, V. G.; Malkina, O. L.; Salahub, D. R. *Chem. Phys. Lett.* **1995**, *235*, 382−388.

(78) Kaupp, M.; Malkin, V. G.; Malkina, O. L.; Salahub, D. R. *Chem.− Eur. J.* **1996**, *2*, 24−30.

D_2O) 9.14 (d, $J = 6.5$ Hz, 12H, $H_{\alpha-py}$), 8.38 (m, 6H, H_3, $H_{3'}$, bipy), 8.28 (m, 6H, H_4, $H_{4'}$, bipy), 7.81 (d, $J = 6$ Hz, 12H, $H_{\beta-py}$), 7.73 (d, $J = 5.5$ Hz, 6H, H_6, $H_{6'}$, bipy), 7.53 (m, 6H, H_5, $H_{5'}$, bipy); ^{19}F NMR (376.5, D_2O) −143.15 (s, $F_{\mathbf{A}}$). **(1aA)$_4$/(1aA)$_3$**: Anal. Calcd for $(C_{26}H_{16}F_4N_6O_6Pd)_n$ ($M_r(n) = 690.86$): C, 45.20; H, 2.31; N, 12.16. Found: C, 45.37; H, 2.41; N, 12.24. ν_{max}(KBr)/cm^{-1}: 1595, 1467, 980 (**A**), 1548, 769 (bipy), 1383, 823 (NO_3).

Square/Triangle (1bA)$_4$/(1bA)$_3$. To a prewarmed (60 °C) solution of $[Pt(NO_3)_2(bipy)]$ (15 mg, 0.03 mmol) in H_2O (4 mL) was added dropwise a solution of 1,4-bis(4-pyridyl)tetrafluorobenzene (**A**) (10 mg, 0.03 mmol) in MeOH (8 mL) at the same temperature. After 72 h of refluxing, ^{1}H NMR spectroscopy showed maximum conversion. The solvent was evaporated to dryness yielding a yellowish solid that was characterized. **(1bA)$_4$**: ^{1}H NMR (400.1 MHz, D_2O) 9.20 (br, 16H, $H_{\alpha-py}$), 8.40 (br, 8H, H_3, $H_{3'}$, bipy), 8.33 (br, 8H, H_4, $H_{4'}$, bipy), 7.97 (br, 8H, H_5, $H_{5'}$, bipy), 7.91 (br, 16H, $H_{\beta-py}$), 7.57 (br, 8H, H_6, $H_{6'}$, bipy); ^{19}F NMR (376.5 MHz, D_2O) −142.81 (s, $F_{\mathbf{A}}$). **(1bA)$_3$**: ^{1}H NMR (400.1 MHz, D_2O) 9.15 (br, 12H, $H_{\alpha-py}$), 8.40 (br, 6H, H_3, $H_{3'}$, bipy), 8.33 (br, 6H, H_4, $H_{4'}$, bipy), 7.97 (br, 6H, H_5, $H_{5'}$, bipy), 7.81 (br, 12H, $H_{\beta-py}$), 7.64 (br, 6H, H_6, $H_{6'}$, bipy); ^{19}F NMR (376.5 MHz, D_2O) −142.99 (s, $F_{\mathbf{A}}$). **(1bA)$_4$/(1bA)$_3$**: ν_{max}(KBr)/cm^{-1} 1615, 1474, 984 (**A**), 1548, 776 (bipy), 1383, 829 (NO_3).

Square/Triangle (1cA)$_4$/(1cA)$_3$. 1,4-Bis(4-pyridyl)tetrafluorobenzene (**A**) (10 mg, 0.03 mmol) and $[Pd(OTf)_2(bipy)]$ (**1c**) (18 mg, 0.03 mmol) were reacted and worked up as described for **(1aA)$_4$/(1aA)$_3$** to yield 17 mg (65%) of a yellowish solid. **(1cA)$_4$**: ^{1}H NMR (400.1 MHz, CD_3NO_2) 9.45 (d, $J = 6.7$ Hz, 16H, $H_{\alpha-py}$), 8.43 (br, 16H, H_3, $H_{3'}$, H_4, $H_{4'}$, bipy), 8.03 (d, 16H, $J = 5.9$ Hz, $H_{\beta-py}$), 7.64 (br, 16H, H_5, $H_{5'}$, H_6, $H_{6'}$, bipy); ^{19}F NMR (376.5 MHz, CD_3NO_2) −143.25 (s, $F_{\mathbf{A}}$). **(1cA)$_3$**: ^{1}H NMR (400.1 MHz, CD_3NO_2) 9.37 (d, $J = 6.7$ Hz, 12H, $H_{\alpha-py}$), 8.43 (br, 12H, H_3, $H_{3'}$, H_4, $H_{4'}$, bipy), 7.95 (d, 12H, $J = 5.6$ Hz, $H_{\beta-py}$), 7.64 (br, 12H, H_5, $H_{5'}$, H_6, $H_{6'}$, bipy); ^{19}F NMR (376.5 MHz, CD_3NO_2) −143.20 (s, $F_{\mathbf{A}}$). **(1cA)$_4$/(1cA)$_3$**: Anal. Calcd for $(C_{28}H_{16}F_{10}N_4O_6PdS_2)_n$ ($M_r(n) = 864.99$): C, 38.88; H, 1.86; N, 6.48. Found: C, 38.77; H, 1.71; N, 6.34. ν_{max}(KBr)/cm^{-1}: 1608, 1470, 987 (**A**), 1545, 775 (bipy), 1262, 1170, 1038 (OTf).

Square/Triangle (1dA)$_4$/(1dA)$_3$. Solid 1,4-bis(4-pyridyl)tetrafluorobenzene (**A**) (5 mg, 0.02 mmol) was added to a CH_3NO_2 (5 mL) solution of $[Pt(OTf)_2(bipy)]$ (**1d**) (12 mg, 0.02 mmol) at room temperature. After 4 h of stirring, the resulting solution was taken to dryness in vacuo and a brownish solid was obtained 15 mg (80%). **(1dA)$_4$**: ^{1}H NMR (400.1 MHz, CD_3NO_2) 9.43 (d, $J = 6.8$ Hz, 16H, $H_{\alpha-py}$), 8.57 (m, 8H, H_3, $H_{3'}$, bipy), 8.49 (m, 8H, H_4, $H_{4'}$, bipy), 8.04 (d, $J = 6.4$ Hz, 16H, $H_{\beta-py}$), 7.87 (br, 8H, H_6, $H_{6'}$, bipy), 7.75 (br, 8H, H_5, $H_{5'}$, bipy); ^{19}F NMR (376.5 MHz, CD_3NO_2) −144.10 (s, F_A). **(1aA)$_3$**: ^{1}H NMR (400.1 MHz, CD_3NO_2) 9.35 (d, $J = 6.8$ Hz, 12H, $H_{\alpha-py}$), 8.58 (m, 6H, H_3, $H_{3'}$, bipy), 8.50 (br, 6H, H_4, $H_{4'}$, bipy), 8.21 (br, 6H, H_6, $H_{6'}$, bipy), 7.95 (d, $J = 6.4$ Hz, 12H, $H_{\beta-py}$), 7.76 (br, 6H, H_5, $H_{5'}$, bipy); ^{19}F NMR (376.5, CD_3NO_2) −144.18 (s, F_A). **(1dA)$_4$/(1dA)$_3$**: Anal. Calcd for $(C_{28}H_{16}F_{10}N_4O_6PtS_2)_n$ ($M_r(n) = 953.65$): C, 35.26; H, 1.69; N, 5.87. Found: C, 35.22; H, 1.71; N, 5.74. ESI-MS (m/z): 1757.1 ($[$**(1dA)$_4$** $-$ 2OTf$]^{2+}$, $[Pt_2(bipy)_2\mathbf{A}_2(OTf)_3]^+$), 1280.6 ($[$**(1dA)$_3$** $-$ 2OTf$]^{2+}$, $[$**(1dA)$_3$** $-$ 2OTf$]_2^{4+}$), 1121.7 $[$**(1dA)$_4$** $-$ 3OTf$]^{3+}$, 804.1 ($[$**(1dA)$_4$** $-$ 4OTf$]^{4+}$, $[$**(1dA)$_3$** $-$ 3OTf$]^{3+}$, $[Pt_2(bipy)_2\mathbf{A}_2(OTf)_2]^{2+}$, $[Pt(bipy)\mathbf{A}(OTf)]^+$), 613.4 $[$**(1dA)$_4$** $-$ 5OTf$]^{5+}$, 565.8 $[$**(1dA)$_3$** $-$ 4OTf$]^{4+}$, 486.4 $[$**(1dA)$_4$** $-$ 6OTf$]^{6+}$, 422.8 $[$**(1dA)$_3$** $-$ 5OTf$]^{5+}$. ν_{max}(KBr)/cm^{-1}: 1588, 985, 824, (**A**); 1549, 775 (bipy); 1261, 1170, 1036 (OTf).

Square/Triangle (2cA)$_4$/(2cA)$_3$. 1,4-Bis(4-pyridyl)tetrafluorobenzene (**A**) (10 mg, 0.03 mmol) and $[Pd(OTf)_2(4,4'\text{-}Me_2bipy)]$ (**2c**) (10 mg, 0.03 mmol) were reacted and worked up as described for **(1aA)$_4$/(1aA)$_3$** to yield 24 mg (83%) of a greenish solid. **(2cA)$_4$**: ^{1}H NMR (400.1 MHz, CD_3NO_2) 9.43 (d, $J = 6.5$ Hz, 16H, $H_{\alpha-py}$), 8.33(s, 8H, H_3, $H_{3'}$, Me_2bipy), 8.01 (d, $J = 6.5$ Hz, 16H, $H_{\beta-py}$), 7.46 (d, $J = 7$ Hz, 8H, H_5, $H_{5'}$, Me_2bipy), 7.40 (d, $J = 6.5$ Hz, 8H, H_6, $H_{6'}$, Me_2bipy), 2.65 (s, 24H, $-CH_3$, Me_2bipy); ^{19}F NMR (376.5 MHz, CD_3NO_2) −143.45 (s, F_A). **(2cA)$_3$**: ^{1}H NMR (400.1 MHz, CD_3NO_2) 9.35 (d, $J = 6.5$ Hz, 12H, $H_{\alpha-py}$), 8.34 (s, 6H, H_3, $H_{3'}$, Me_2bipy), 7.91 (d, $J = 7$ Hz, 12H, $H_{\beta-py}$), 7.77 (d, $J = 6$ Hz, 6H, H_6, $H_{6'}$, Me_2bipy), 7.51 (d, $J = 5$ Hz, 6H, H_5, $H_{5'}$, Me_2bipy), 2.67 (s, 18H, -CH_3, Me_2bipy); ^{19}F NMR (376.5 MHz, CD_3NO_2) −143.40 (s, F_A). **(2cA)$_4$/(2cA)$_3$**: Anal. Calcd for $(C_{30}H_{20}F_{10}N_4O_6PdS_2)_n$ ($M_r(n) = 893.04$): C, 40.35; H, 2.26; N, 6.27. Found: C, 40.27; H, 2.16; N, 6.12. ESI-MS (m/z): 1636.0 ($[$**(2cA)$_4$** $-$ 2OTf$]^{2+}$, $[Pd_3(4,4'\text{-}Me_2bipy)_2\mathbf{A}_2(OTf)_3]^+$), 1190.0 $[$**(2cA)$_3$** $-$ 2OTf$]^{2+}$, 1042.3 $[$**(2cA)$_4$** $-$ 3OTf$]^{3+}$, 1038.0 $[Pd_3(4,4'\text{-}Me_2bipy)_3\mathbf{A}_2(OTf)_4]^{2+}$, 744.0 $[Pd(4,4'\text{-}Me_2bipy)\mathbf{A}OTf]^+$. ν_{max}(KBr)/cm^{-1}: 1618, 1476, 983 (**A**), 1622, 516 (4,4′-Me_2bipy), 1258, 1159, 1029 (OTf).

Square/Triangle (3aA)$_4$/(3aA)$_3$. 3a was synthesized in situ by addition of 17 mg (0.06 mmol) of solid AgOTf to a CH_2Cl_2 (15 mL) solution of $[PdCl_2(4,4'\text{-}t\text{-}Bu_2bipy)]$(14 mg, 0.03 mmol). The reaction mixture was stirred for 24 h with exclusion of light. After filtration, the resulting solution was concentrated in vacuo and an oily compound was obtained. Then, solid 1,4-bis(4-pyridyl)-tetrafluorobenzene (**A**) (10 mg, 0.03 mmol) was added to a CH_2Cl_2 (7 mL) solution of $[Pd(OTf)_2(4,4'\text{-}t\text{-}Bu_2bipy)]$. After 12 h of stirring, a gray solid precipitated. Filtration and drying in vacuo gave 11 mg (35%) of the desired product. **(3aA)$_4$**: ^{1}H NMR (400.1 MHz, CD_3NO_2) 9.43 (d, $J = 6.7$ Hz, 16H, $H_{\alpha-py}$), 8.51(br, 8H, H_3, $H_{3'}$, *t*-Bu_2bipy), 8.03 (d, $J = 5.7$ Hz, 16H, $H_{\beta-py}$), 7.66 (m, 8H, H_5, $H_{5'}$, *t*-Bu_2bipy), 7.46 (d, $J = 6.2$ Hz, 8H, H_6, $H_{6'}$, *t*-Bu_2bipy), 1.44 (s, 72H, $-C(CH_3)_3$, *t*-Bu_2bipy); ^{19}F NMR (376.5 MHz, CD_3NO_2) −142.55 (s, F_A). **(3aA)$_3$**: ^{1}H NMR (400.1 MHz, CD_3NO_2) 9.35 (d, $J = 6.5$ Hz, 12H, $H_{\alpha-py}$), 8.52 (br, 6H, H_3, $H_{3'}$, *t*-Bu_2bipy), 7.94 (d, $J = 6$ Hz, 12H, $H_{\beta-py}$), 7.85 (d, $J = 6.0$ Hz, 6H, H_6, $H_{6'}$, *t*-Bu_2bipy), 7.68 (m, 6H, H_5, $H_{5'}$, *t*-Bu_2bipy), 1.45 (s, 54H, $-C(CH_3)_3$, *t*-Bu_2bipy); ^{19}F NMR (376.5 MHz, CD_3NO_2) −142.52 (s, F_A). **(3aA)$_4$/(3aA)$_3$**: Anal. Calcd for $(C_{36}H_{32}F_{10}N_4O_6PdS_2)_n$ ($M_r(n) = 977.21$): C, 44.25; H, 3.30; N, 5.73. Found: C, 43.95; H, 3.26; N, 5.63. ESI-MS (m/z): 1805.0 $[$**(3aA)$_4$** $-$ 2OTf$]^{2+}$, $[Pd_2(4,4'\text{-}t\text{-}Bu_2bipy)_2\mathbf{A}_2(OTf)_3]^+$), 1316.5 $[$**(3aA)$_3$** $-$ 2OTf$]^{2+}$, 1164.4 $[Pd_3(4,4'\text{-}t\text{-}Bu_2bipy)_3\mathbf{A}_2(OTf)_4]^{2+}$, 1153.7 $[$**(3aA)$_4$** $-$ 3OTf$]^{3+}$, 827.1 $[Pd(4,4'\text{-}t\text{-}Bu_2bipy)\mathbf{A}OTf]^+$. ν_{max}(KBr)/cm^{-1}: 1619, 1476, 983 (**A**), 2960, 1277 (4,4′-*t*-Bu_2bipy), 1257, 1160, 1030 (OTf).

Square/Triangle (3bA)$_4$/(3bA)$_3$. 1,4-Bis(4-pyridyl)tetrafluorobenzene (**A**) (10 mg, 0,03 mmol) and $[Pt(OTf)_2(4,4'\text{-}tBu_2bipy)]$ (**3b**) (25 mg, 0.03 mmol) were reacted and worked up as described for **(1aA)$_4$/(1aA)$_3$** to yield 11 mg (30%) of a brown solid. **(3bA)$_4$**: ^{1}H NMR (400.1 MHz, CD_3NO_2) 9.41 (d, $J = 6$ Hz, 16H, $H_{\alpha-py}$), 8.53 (s, 8H, H_3, $H_{3'}$, *t*-Bu_2bipy), 8.03 (d, $J = 5.5$ Hz, 16H, $H_{\beta-py}$), 7.72 (br, 16H, H_5, $H_{5'}$, H_6, $H_{6'}$, *t*-Bu_2bipy), 1.46 (s, 72H, -$C(CH_3)_3$, *t*-Bu_2bipy); ^{19}F NMR (376.5 MHz, CD_3NO_2) −146.40 (s, F_A). **(3bA)$_3$**: ^{1}H NMR (400.1 MHz, CD_3NO_2) 9.32 (d, $J = 6.6$ Hz, 12H, $H_{\alpha-py}$), 8.53 (s, 6H, H_3, $H_{3'}$, *t*-Bu_2bipy), 7.94 (d, $J = 6.5$ Hz, 12H, $H_{\beta-py}$), 7.72 (s, 12H, H_5, $H_{5'}$, H_6, $H_{6'}$, *t*-Bu_2bipy), 1.47 (s, 72H, $-C(CH_3)_3$, *t*-Bu_2bipy); ^{19}F NMR (376.5 MHz, CD_3NO_2) −146.24 (s, F_A). **(3bA)$_4$/(3bA)$_3$**: Anal. Calcd for $(C_{36}H_{32}F_{10}N_4O_6PtS_2)_n$ ($M_r(n) = 1065.87$): C, 40.57; H, 3.03; N, 5.26. Found: C, 40.77; H, 3.05; N, 5.13. ESI-MS (m/z): 1981.3 ($[$**(3bA)$_4$** $-$ 2OTf$]^{2+}$, $[Pt_2(4,4'\text{-}t\text{-}Bu_2bipy)_2\mathbf{A}_2(OTf)_3]^+$), 1715.0 ($[$**(3bA)$_4$(3bA)$_3$** $-$ 4OTf$]^{4+}$), 1448.8 $[$**(3bA)$_3$** $-$ 2OTf$]^{2+}$, 1271.2 $[$**(3bA)$_4$** $-$ 3OTf$]^{3+}$, 1220.3 $[Pt(4,4'\text{-}t\text{-}Bu_2bipy)A_2(OTf)]^+$, 916.2 ($[$**(3bA)$_4$** $-$ 4OTf$]^{4+}$, $[$**(3bA)$_3$** $-$ 3OTf$]^{3+}$,

Scheme 1

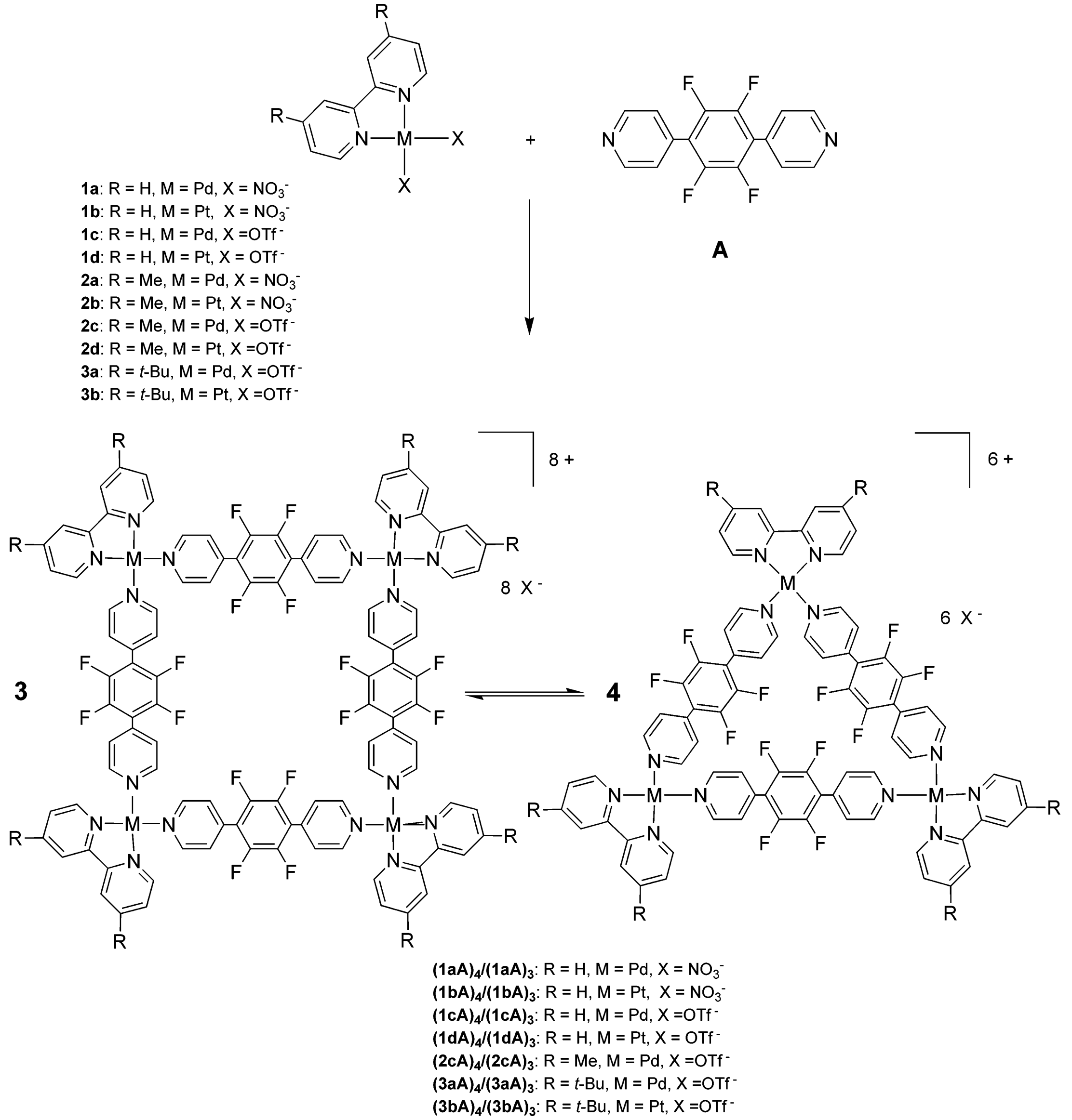

1a: R = H, M = Pd, X = NO_3^-
1b: R = H, M = Pt, X = NO_3^-
1c: R = H, M = Pd, X = OTf^-
1d: R = H, M = Pt, X = OTf^-
2a: R = Me, M = Pd, X = NO_3^-
2b: R = Me, M = Pt, X = NO_3^-
2c: R = Me, M = Pd, X = OTf^-
2d: R = Me, M = Pt, X = OTf^-
3a: R = *t*-Bu, M = Pd, X = OTf^-
3b: R = *t*-Bu, M = Pt, X = OTf^-

$(1aA)_4/(1aA)_3$: R = H, M = Pd, X = NO_3^-
$(1bA)_4/(1bA)_3$: R = H, M = Pt, X = NO_3^-
$(1cA)_4/(1cA)_3$: R = H, M = Pd, X = OTf^-
$(1dA)_4/(1dA)_3$: R = H, M = Pt, X = OTf^-
$(2cA)_4/(2cA)_3$: R = Me, M = Pd, X = OTf^-
$(3aA)_4/(3aA)_3$: R = *t*-Bu, M = Pd, X = OTf^-
$(3bA)_4/(3bA)_3$: R = *t*-Bu, M = Pt, X = OTf^-

[Pt(4,4′-*t*-Bu_2bipy)**A**OTf]$^+$). ν_{max}(KBr)/cm^{-1}: 1622, 1478, 985 (**A**), 2980, 1278 (4,4′-*t*-Bu_2bipy), 1258, 1160, 1030 (OTf).

Square (4aA)$_4$. Solid 1,4-bis(4-pyridyl)tetrafluorobenzene (**A**) (50 mg, 0.16 mmol) was added to a H_2O/MeOH/EtOH (1/3/3 mL) solution of [Pd(NO_3)$_2$(en)] **(4a)** (47 mg, 0.16 mmol) at room temperature. After 4 h of stirring, the resulting solution was taken to dryness in vacuo and 78 mg (82%) of a brown solid was obtained. ^{1}H NMR (400.1 MHz, D_2O): 8.91 (d, $J = 6.4$ Hz, 16 H, $H_{\alpha-py}$), 7.82 (d, $J = 6.4$ Hz, 16 H, $H_{\beta-py}$), 2.94 (s, 16H, $-CH_2$); ^{19}F NMR (376.5 MHz, D_2O): −145.3 (s, F_A). Anal. Calcd for $C_{72}H_{64}F_{16}N_{24}O_{24}Pd_4$: C, 36.35; H, 2.71; N, 14.13. Found: C, 35.98; H, 2.68; N, 14.29. ν_{max}(KBr)/cm^{-1}: 3437 (en), 1619, 1475, 981, 822 (**A**), 1384, 815 (NO_3).

Square (4bA)$_4$. Solid [Pt(NO_3)$_2$(en)] (**4b**) (46 mg, 0.12 mmol) and solid 1,4-bis(4-pyridyl)tetrafluorobenzene (**A**) (37 mg, 0.12 mmol) were mixed in an agate mortar (20 min approximately), and then, pressure was applied (500 MPa) to a tablet of the obtained powder during 10 min. Changes in both color and texture of the solid were indicative of a reaction was taken place. Monitoring by ^{1}H NMR was necessary to confirm reaction completion. Usually, the above-described operations have to be repeated several times to obtain a brown solid in nearly quantitative yield. ^{1}H NMR (400.1 MHz, D_2O): 8.84 (d, $J = 5.7$ Hz, 16 H, $H_{\alpha-py}$), 7.70 (d, $J = 5.7$ Hz, 16 H, $H_{\beta-py}$), 2.73 (s, 16H, $-CH_2$); ^{19}F NMR (376.5 MHz, D_2O): −145.2 (s, F_A). Anal. Calcd for $C_{72}H_{64}F_{16}N_{24}O_{24}Pt_4$: C, 31.63; H, 2.36; N, 12.30. Found: C, 31.58; H, 2.39; N, 12.22. ν_{max}(KBr)/cm^{-1}: 1623, 1478, 980, 819 (**A**) 1384, 815 (NO_3).

Square (4cA)$_4$. A solution of NH_4PF_6 (274 mg, 1.68 mmol) in 30 mL of water was added to a aqueous solution of **(4aA)$_4$** (33 mg, 0.014 mmol) at room temperature. After 2 h of stirring, a yellowish solid precipitated. Filtration and drying in vacuum gave 28 mg (66%) of the product. ^{1}H NMR (400.1 MHz, CD_3NO_2): 9.04 (d, $J = 5.9$ Hz, 16H, $H_{\alpha-py}$), 7.78 (d, $J = 5.9$ Hz, 16H, $H_{\beta-py}$), 3.14 (s, 16H, $-CH_2$); ^{19}F NMR (376.5 MHz, CD_3NO_2): 73.8 (d, $J = 708$ Hz, 48F, PF_6), −144.2 (s, 16F, F_A). Anal. Calcd for $C_{72}H_{64}F_{64}N_{16}P_8Pd_4$: C, 28.42; H, 2.12; N, 7.36. Found: C, 29.02; H, 2.21; N, 7.29. ν_{max}(KBr)/cm^{-1}: 1618, 1476, 984 (**A**), 1555, 845 (PF_6).

Results and Discussion

Self-Assembly Reactions Involving Bipyridine Compounds. Scheme 1 summarizes the self-assembly reactions performed with compounds **1a−d**, **2a−d**, and **3a**,**b**.

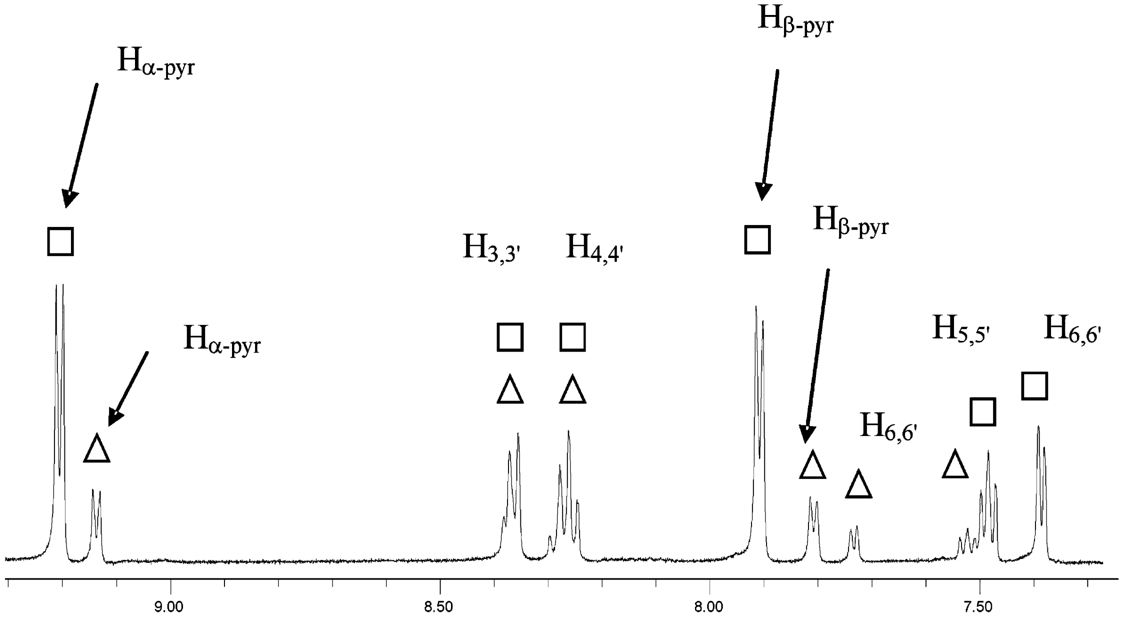

Figure 1. Aromatic region of the ^{1}H NMR spectrum of **(1aA)$_4$/(1aA)$_3$** in D_2O.

Although using a series of metallic precursors with different R groups and/or counteranions (nitrate or triflate) ensured diverse solubility properties in both the building blocks and the formed macrocycles, some of the combinations (see below) did not give the desired metallomacrocycles.

As a starting point, we treated a 1:1 MeOH/H_2O solution of [Pd(NO_3)$_2$(2,2′-bipy)] (**1a**) with 1 equiv of solid **A** under the same conditions reported by Fujita et al.[50] in their studies using 4,4′-bipyridine as organic edge. However, NMR analysis of the resulting yellow solution revealed a complex mixture of species that could not be identified. After several attempts, we found that by mixing equimolar amounts of **1a** and **A** in CH_2Cl_2 at room temperature, a yellowish solid gradually formed, which was then filtered off and washed with the same solvent. Since the insolubility of the product in the reaction solvent precluded monitoring by NMR spectroscopy, we dissolved the precipitate in D_2O and recorded the corresponding spectra.

The ^{1}H NMR spectrum (Figure 1) indicates the presence of two symmetric components, which we assigned to the square and triangular species **(1aA)$_4$/(1aA)$_3$**. The molecular square resulted to be predominant over the triangle within the range of studied concentrations. Figure 1 shows two sets of peaks assignable to the α and β protons of the pyridine rings, as well as two differentiated sets of signals for each type of proton ($H_{3,3'}$, $H_{4,4'}$, $H_{5,5'}$, and $H_{6,6'}$) of the 2,2′-bipyridine ligands whose assignment is based on g-COSY 2D and TOCSY 1D NMR experiments (see Supporting Information). Interestingly, the aromatic protons $H_{5,5'}$ and $H_{6,6'}$ of the 2,2′-bipy have shifted upfield ($\Delta\delta_{\text{range}} = 0.87-0.20$ ppm), suggesting that they may have experienced ring currents from the adjacent pyridine ligands resulting from metallocycle formation. Moreover, this shielding is larger in the square, since an increase in the N(py)−Pd−N(py) angle provokes a major proximity between the aromatic rings of **A** and the 2,2′-bipyridine ligand. This effect result was remarkable for $H_{6,6'}$, in which a variation of 0.35 ppm between the corresponding square and triangle protons was observed. To justify these spectroscopic data theoretically, a GIAO-DFT study was carried out (see below).

According to the ^{1}H NMR spectrum, the ^{19}F NMR exhibited a pair of very close singlets (−142.90 and −143.15 ppm) consistent with the formation of **(1aA)$_4$/(1aA)$_3$** in solution.

To confirm the ring size of the macrocycles an ESI-MS analysis was undertaken. Given that no informative signals were obtained for the nitrate derivatives **(1aA)$_4$/(1aA)$_3$**, we decided to synthesize the analogous triflate compounds **(1cA)$_4$/(1cA)$_3$** under the same conditions described above. Their CD_3NO_2 NMR spectra were very similar to that of **(1aA)$_4$/(1aA)$_3$**. Unfortunately, the ESI-MS spectrum in nitromethane or acetone failed to show neither triangles nor squares and the only detected metal species was the mononuclear [Pd(bipy)**A**(OTf)]$^+$ (m/z = 715.1). Obviously, the macrocycles present in solution are not stable enough for ionization as intact supramolecules even under the softest ESI conditions used.

To obtain more stable complexes for MS analysis, platinum analogues were prepared. While the nitrate compounds, **(1bA)$_4$/(1bA)$_3$**, required forcing conditions (72 h in refluxing 1:2 H_2O:MeOH), the triflate derivatives, **(1dA)$_4$/(1dA)$_3$**, were obtained by simply mixing equimolar amounts of **1d** and **A** in nitromethane at room temperature. Interestingly, although ^{1}H and ^{19}F NMR experiments always showed the presence of two species, in the case of the nitrate complexes **(1bA)$_4$/(1bA)$_3$**, the molecular triangle resulted to be the predominant species regardless of concentration, in contrast with all of our other experiments in which the square was always the most abundant. Although unexpected, similar behavior has been reported by other authors[48] who observed exclusive formation of the triangle under refluxing conditions, while both the triangle and the square formed at room temperature. This temperature dependence could be explained

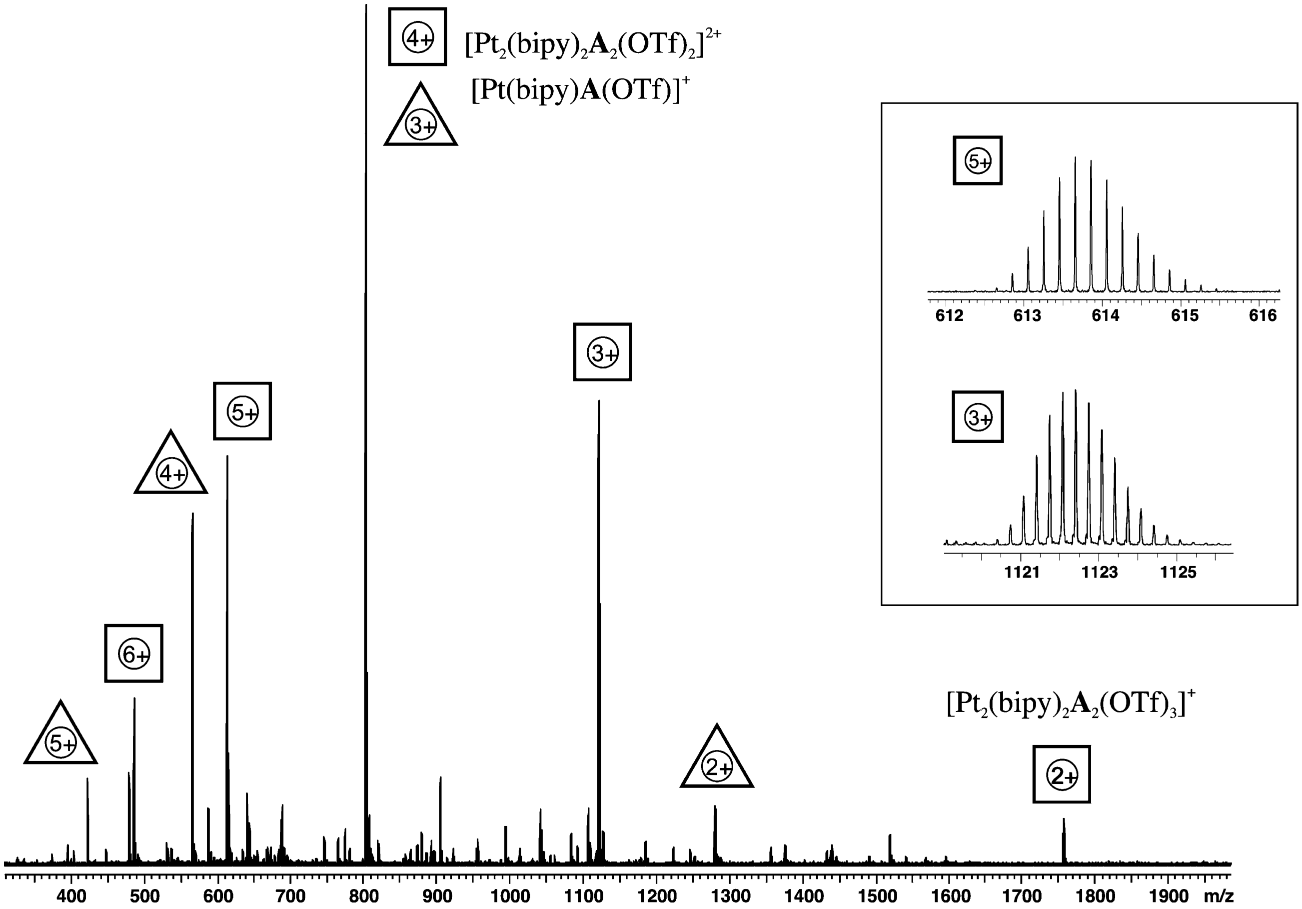

Figure 2. ESI-FT-ICR (nitromethane solution) mass spectrum of the triangle−square equilibrium **(1dA)$_4$/(1dA)$_3$**. The insets show the measured isotope patterns of the penta charged [(**1dA**)$_4$ − 5OTf]$^{5+}$ (top) and triply charged [(**1dA**)$_4$ − 3OTf]$^{3+}$ (bottom) squares.

in terms of a competition between enthalpy and entropy effects. Therefore, under refluxing conditions, entropy effects may be more prominent than enthalpy effects, thus favoring the formation of the more sterically strained triangle over the enthalpically preferred square.

ESI-MS analysis of the more stable platinum complexes showed intact metallomacrocycles only in the triflate derivatives **(1dA)$_4$/(1dA)$_3$**, which unambiguously confirmed the coexistence of both square and triangular species in the studied equilibrium. The resulting mass spectrum, measured from a nitromethane solution (Figure 2), displays multiply charged molecular ions that correspond to the square **(1dA)$_4$** at m/z = 1757.1 [**(1dA)$_4$** − 2OTf]$^{2+}$, 1121.7 [**(1dA)$_4$** − 3OTf]$^{3+}$, 804.1 [**(1dA)$_4$** − 4OTf]$^{4+}$, 613.5 [**(1dA)$_4$** − 5OTf]$^{5+}$, and 486.4 [**(1dA)$_4$** − 6OTf]$^{6+}$. Analogously, the peaks appearing at m/z = 1280.6 [**(1dA)$_3$** − 2OTf]$^{2+}$, 804.1 [**(1dA)$_3$** − 3OTf]$^{3+}$, and 565.8 [**(1dA)$_3$** − 4OTf]$^{4+}$ correspond to the molecular triangle **(1dA)$_3$**. Some of the signals have an experimental isotope pattern resulting from the superposition of several fragments. In particular, the calculated pattern, based on the natural abundances, of the most intense peak in Figure 2 indicates that the signals of the quadruply charged square [**(1dA)$_4$** − 4OTf]$^{4+}$ and the triply charged triangle [**(1dA)$_3$** − 3OTf]$^{3+}$ are superimposed with small amounts of both the doubly charged bimetallic fragment [Pt$_2$(bipy)$_2$**A$_2$**(OTf)$_2$]$^{2+}$ and the monometallic [Pt(bipy)**A**(OTf)]$^+$ (Figure 3).

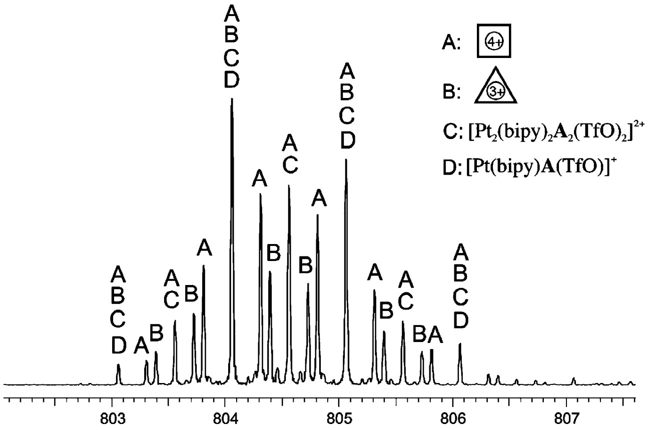

Figure 3. Superimposition of signals arising from the quadruply charged square [(**1dA**)$_4$ − 4OTf]$^{4+}$, the triply charged triangle [(**1dA**)$_3$ − 3OTf]$^{3+}$, the doubly charged bimetallic fragment [Pt$_2$(bipy)$_2$**A$_2$**(OTf)$_2$]$^{2+}$, and the monometallic [Pt(bipy)**A**(OTf)]$^+$.

Self-assembly between nitrate or triflate 4,4′-dimethyl-2,2′-bipyridine corners (**2a**−**d**) and **A** only yielded the expected molecular polygons for the palladium triflate derivative [Pd(OTf)$_2$(4,4′-Me$_2$bipy)] (**2c**), although many attempts were made by varying reaction conditions (solvent, temperature, concentration, and reaction time).

When [Pd(OTf)$_2$(4,4′-Me$_2$bipy)] (**2c**) was combined with **A** in a 1:1 molar ratio in CH$_2$Cl$_2$ at room temperature a greenish solid was formed. ^{1}H and ^{19}F NMR analysis in CD$_3$NO$_2$ solution (see Supporting Information) indicated the

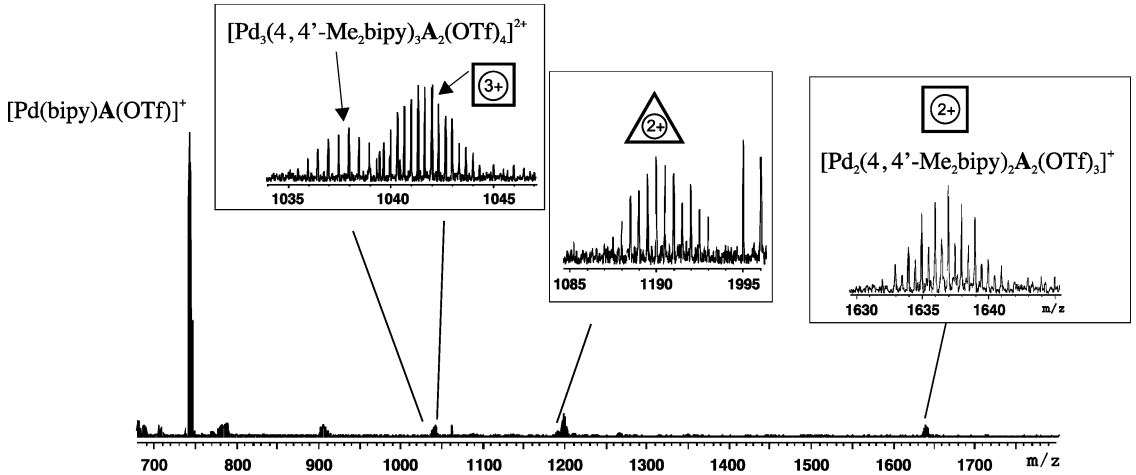

Figure 4. ESI-FT-ICR (nitromethane solution) mass spectrum of the triangle−square equilibrium $(\mathbf{2cA})_4/(\mathbf{2cA})_3$. The insets show the measured isotope patterns of the triply charged square $[(\mathbf{2cA})_4 - 3\mathrm{OTf}]^{3+}$ (left) and the doubly charged triangle $[(\mathbf{2cA})_3 - 2\mathrm{OTf}]^{2+}$ (middle) together with the superimposition of doubly charged tetrameric $[(\mathbf{2cA})_4 - 2\mathrm{OTf}]^{2+}$ and singly charged dimeric species.

presence of two symmetrical species $(\mathbf{2cA})_4/(\mathbf{2cA})_3$ that could be unambiguously assigned to a triangle and a square by means of ESI-FT mass spectrometry. The overview spectrum of this system in nitromethane solution (Figure 4) shows mainly gas-phase fragments but also both the doubly and triply charged squares, $[(\mathbf{2cA})_4 - 2\mathrm{OTf}]^{2+}$, $[(\mathbf{2cA})_4 - 3\mathrm{OTf}]^{3+}$, at $m/z = 1637.0$ and 1042.3 respectively, together with a peak at $m/z = 1190.0$ assignable to the triangle $[(\mathbf{2cA})_3 - 2\mathrm{OTf}]^{2+}$. The signal centered at $m/z = 1637.0$ is a superimposition of doubly charged tetrameric and singly charged dimeric species (inset Figure 4), the latter being the most abundant.

The last studied bipyridine system gave good results for both palladium and platinum compounds. Equimolar amounts of $[\mathrm{M(OTf)_2}(4,4'\text{-}t\text{-}\mathrm{Bu_2bipy})]$ (M = Pd, **3a**; M = Pt, **3b**) and **A** were reacted in $\mathrm{CH_2Cl_2}$ at room temperature to give quantitative yields of solids whose characterization indicated to correspond to the square/triangle mixtures $(\mathbf{3aA})_4/(\mathbf{3aA})_3$ (M = Pd) and $(\mathbf{3bA})_4/(\mathbf{3bA})_3$ (M = Pt). Once again, NMR spectroscopy showed that the square species are predominant within the range of studied concentrations.

ESI-MS analysis provided strong evidence for the formation of the metallomacrocycles. In the nitromethane mass spectrum of $(\mathbf{3aA})_4/(\mathbf{3aA})_3$ (see Supporting information) the peaks appearing at $m/z = 1153.7$, 1316.5, and 1805.0 can be assigned to triply charged square $[(\mathbf{3aA})_4 - 3\mathrm{OTf}]^{3+}$, doubly charged triangle $[(\mathbf{3aA})_3 - 2\mathrm{OTf}]^{2+}$, and a superimposition of $[(\mathbf{3aA})_4 - 2\mathrm{OTf}]^{2+}$ and $[\mathrm{Pd_2}(4,4'\text{-}t\text{-}\mathrm{Bu_2bipy})_2\mathbf{A}_2(\mathrm{OTf})_2]^{+}$, respectively. In the acetone spectrum of the platinum metallomacrocycles $(\mathbf{3bA})_4/(\mathbf{3bA})_3$ (see Supporting Information), the most intense signal corresponds to the square $[(\mathbf{3bA})_4 - 3\mathrm{OTf}]^{3+}$ ($m/z = 1271.3$). Other relevant peaks are the doubly and quadruply charged squares $[(\mathbf{3bA})_4 - 2\mathrm{OTf}]^{2+}$ ($m/z = 1981.3$) and $[(\mathbf{3bA})_4 - 4\mathrm{OTf}]^{4+}$ ($m/z = 916.2$) and the doubly and triply charged triangles $[(\mathbf{3bA})_3 - 2\mathrm{OTf}]^{2+}$ ($m/z = 1448.8$) and $[(\mathbf{3bA})_3 - 3\mathrm{OTf}]^{3+}$ ($m/z = 916.2$), which in some cases are superimposed with species of lower nuclearity. According to previously reported observations,[79] fragmentation resulted to be considerably greater for the palladium compounds $(\mathbf{3aA})_4/(\mathbf{3aA})_3$ than those of the analogous platinum assemblies $(\mathbf{3bA})_4/(\mathbf{3bA})_3$, a fact that evidences the greater stability of the Pt−N bond.

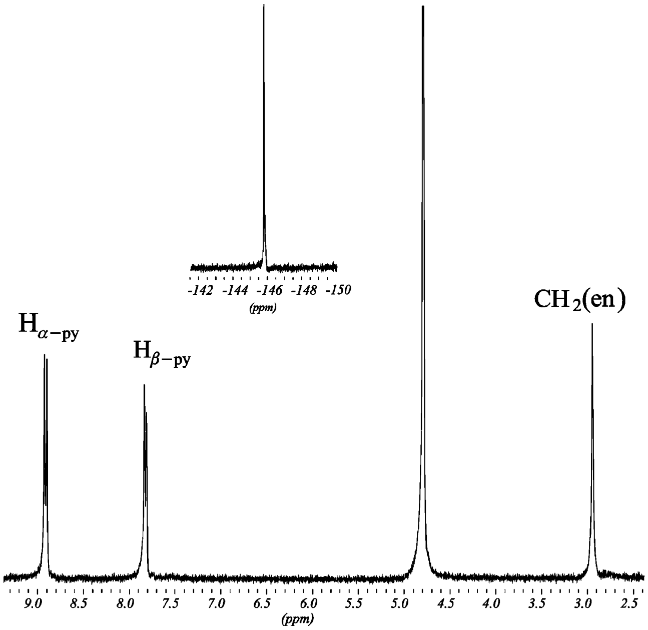

Figure 5. ^{1}H and ^{19}F NMR (inset) spectra of $(\mathbf{4aA})_4$ in $\mathrm{D_2O}$.

Self-Assembly Reactions Involving Ethylenediamine Compounds. The palladium metallomacrocycle $(\mathbf{4aA})_4$ was synthesized by mixing stoichiometric amounts of $[\mathrm{Pd(NO_3)_2(en)}]$ (**4a**) with **A** under conditions similar to those reported by Fujita et al.[53] for the 4,4′-bipy derivative (i.e. room temperature, 1:3:3 $\mathrm{H_2O}$:MeOH:EtOH). In this case, it is remarkable the unexpected formation of one only macrocyclic species $(\mathbf{4aA})_4$, as demonstrated ^{1}H and ^{19}F NMR spectra (Figure 5). Since we were not successful in obtaining either informative ESI-MS spectra or an X-ray crystal structure for this compound, we propose the obtained macrocycle to be a molecular square (Scheme 2) on the basis of literature reports.[8,9,50]

---

(79) Jeong, K. S.; Kim, S. Y.; Shin, U. S.; Kogej, M.; Hai, N. T. M.; Broekmann, P.; Jeong, N.; Kirchner, B.; Reiher, M.; Schalley, C. A. *J. Am. Chem. Soc.* **2005**, *127*, 17672−17685.

Scheme 2

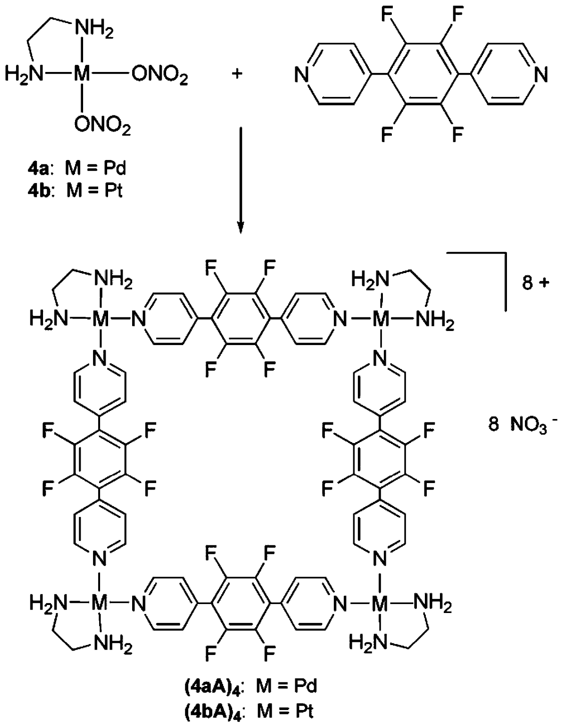

Although many attempts were made using forcing reaction conditions (long reaction times, high temperatures, addition of different salts, etc.), the analogous platinum square **(4bA)$_4$** could not be obtained by mixing the required building blocks in a solvent. However, it was successfully synthesized by grounding and pressing a powdered 1:1 mixture of **4b** and **A** in the absence of solvent.[54] The process was interrupted when a complete change of both color and texture of the mixed solids was observed. NMR spectra of the resulting solid in D_2O showed a very simple pattern consistent with the formation of only one symmetrical structure.

To our knowledge, compound **(4aA)$_4$** and the 4,4′-bipyridine square reported by Fujita et al. are the unique examples in which the self-assembly reaction between the metallic corner $[Pd(NO_3)_2(en)]$ and a ditopic bipyridyl ligand leads to the formation of square species exclusively.[80] It is worth noting that the same authors reported[50] the obtention of square/triangle equlibria when 4,4′-bipyridine is replaced by a longer chain bridging ligand. In particular, the fact that 1,4-bis(4-pyridyl)benzene (nonfluorinated compound analogous to **A**) yielded nonnegligible quantities of triangular compound (70:30 square:triangle, [Pd] = 2 mM) seemed to indicate that the presence of fluorine atoms on the central ring of the organic edge has an important effect on shifting the equilibrium to the exclusive formation of the square species.

To interpret the obtained results theoretically, we have performed molecular mechanics calculations with Cerius2 code using the UFF force field.[81] The analysis of the relative stability of compounds **(4aA)$_4$/(4aA)$_3$** in comparison with their nonfluorinated counterparts showed the fluorinated square **(4aA)$_4$** to be 12 kcal/mol per edge more stable than triangular **(4aA)$_3$** while this stabilization was only of 6.6 kcal/mol between the nonfluorinated species. Although this result is in agreement with the experimental facts, it seems clear that other factors also have an influence on the formation of a determinate species from a self-assembly process.

Table 1. Measured Diffusion Coefficients (*D*) in D_2O and Calculated Hydrodynamic Radii (r_H) from the Stokes−Einstein Equation for **(1aA)$_4$** and **(1aA)$_3$**

compd	diffusion coeff (*D*) (10^{-10} m^2/s, 298 K)	hydrodynamic radius (r_H) (Å)
(1aA)$_4$	1.78	10.8
(1aA)$_3$	2.12	9.0

DOSY Measurements. Since the palladium bipyridine system, **(1aA)$_4$/(1aA)$_3$**, resisted characterization by mass spectrometry, we decided to examine the size of the species by diffusion ordered NMR spectroscopy (DOSY) with ^{1}H detection. The observed values are presented in Table 1.

To compare the expected size of our molecules with the results from the diffusion experiments, we have used molecular modeling. A value of 16 Å resulted from the optimized structure (Cerius2 program, UFF) of the square species **(1aA)$_4$** that does not agree very well with the experimental value (10.8 Å).

In an alternative approach, we evaluated the relative size by approximating the molecules as encapsulating spheres[82] from which the hydrodynamic radius can be calculated by means of purely geometrical considerations. Taking into account that both square and triangle have the same edge length, the ratio between the respective r_H has to be equal to 0.8. As can be deduced from data in Table 1, this value is now in good agreement with the obtained results from DOSY measurements.

Determination of Chemical Shifts by GIAO-DFT Calculations. As reported above, formation of the diimine metallomacrocycles induces the aromatic protons of 2,2′-bypiridine to shift upfield in the ^{1}H NMR spectra, compared with the metallic corner. Moreover, this effect is notably more pronounced for the square than for the triangular derivative. To theoretically analyze this trend, we performed a GIAO-DFT study (see Computational Details) on the model compound (Figure 6).

The calculated chemical shifts for the model complex are shown in Figure 6. It is worth noting the important changes, even in the order, of the chemical shifts between the free and coordinated 2,2′-bipyridine ligand. For the coordinated ligand, there is a continuous decrease in the chemical shift when the N−Pt−N bond angle increases. This fact is especially important for the H_6 protons, which display the largest difference (experimental value = 0.35 ppm) between the corresponding square and triangle shifts. For the other protons, the chemical shifts are very similar for both the square and the triangle structures as predicted with the small change of the shifts with the N−Pt−N angle.

---

(80) Lindoy, L. F.; Atkinson, I. M. *Self-Assembly in Supramolecular Systems*; Royal Society of Chemistry: Cambridge, U.K., 2000.

(81) *Cerius2*, version 3.8; Molecular Simulations: San Diego, CA, 1998.

(82) Otto, W. H.; Keefe, M. H.; Splan, K. E.; Hupp, J. T.; Larive, C. K. *Inorg. Chem.* **2002**, *41*, 6172−6174.

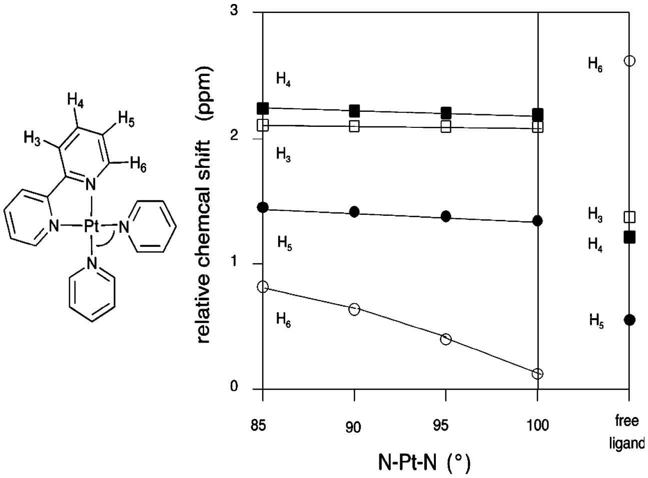

Figure 6. Calculated GIAO values for the model complex (left) corresponding to the relative variation of ^{1}H NMR chemical shifts of the coordinated 2,2′-bipyridine as a function of the N−Pt−N angle value. The calculated chemical shifts of free 2,2′-bipyridine are represented on the right line of the graphics.

These theoretical results are in very good agreement with the above pointed out influence of the aromatic ring current from the **A** pyridine moieties on the nearest 2,2′-bipyridine protons (i.e., 6 and 6′; see Figure 1).

The calculated chemical shifts are obtained from two contributions, the paramagnetic term, whose changes could be rationalized using the molecular orbitals, and the diamagnetic contribution, which depends on several factors.[83] The analysis of the variations indicates that the paramagnetic contribution is only responsible for 20% of the changes in the chemical shifts, which does not allow explaining such variations by using the molecular orbitals.

To verify the hypothesis mentioned above about the influence of the ring current of the bridging ligand on the large change of the chemical shift of the $H_{6,6'}$ proton of the terminal bipyridine ligand, we performed calculations of the nucleus independent chemical shift (NICS) parameter for a simple model.[84] We have just included the one pyridine ring of the bridging ligand, and we have estimated the NICS value at the position of the closest $H_{6,6'}$ proton for the different N−Pt−N bond angles. The results show a constant decrease of the NICS value from −1.11 for model corresponding to the structure with a N−Pt−N angle value of 80° to −2.17 for an angle of 100°. Hence, the larger NICS obtained for larger angle value corroborates that the reduction of the calculated chemical shifts of the $H_{6,6'}$ protons shown in Figure 6 and the assignment of the peaks to the square and triangle complexes in the NMR spectra (Figure 1) is mainly due to the ring current produced by the pyridine ring of the bridging ligand.

Host−Guest Binding Properties. Since cavities of variable sizes are accessible with molecular polygons, selective complexation of organic molecules and ions could be achieved.

Considering the positive charge and the geometry of our macrocycles (square or triangular) and following up on earlier findings that cationic Pd or Pt compounds possessing a fluorinated aromatic function can very effectively encapsulate electron-rich aromatic guests,[85,86] we began our experiments by using the **(1aA)$_4$/(1aA)$_3$** system as a host. Although it was not possible to obtain a clear solution for the latter macrocycles in D_2O, due to hydrolysis, the presence of an approximately equimolar amount of the electron-rich compounds 1,4-dimethoxybenzene (**I**) or 1,3,5-trimethoxybenzene (**II**) failed to yield any indication of encapsulation of the aromatic compound within the square and/or triangle cavities since ^{1}H NMR signals were hardly affected ($\Delta\delta \leq 0.1$ ppm). To get rid of undesirable hydrolysis processes, we performed the experiment with the triflate derivatives **(1cA)$_4$/(1cA)$_3$** in nitromethane, but they did not interact either, as shown by unaffected peaks in NMR spectra.

An anionic guest like sodium 4-methyl-benzoate (**III**) was also investigated. In all cases, however, we observed the immediate formation of a white precipitate, which for NO_3^- derivatives corresponded to a mixture of free **A** and unidentified palladium species (formed by substitution of **A** by the more nucleophile carboxylate anion and subsequent cleavage of the macrocycles). In the case of triflate compounds, NMR spectra from the resulting nitromethane-d_3 solution confirmed the presence of free **A**.

Fortunately, we obtained better results with pure squares **(4aA)$_4$**. When **I**, **II**, or **III** was added to a D_2O solution of either **(4aA)$_4$** ([square] = [organic compound] = 5 mM), upfield shifts in ^{1}H NMR were observed for those signals from aromatic compounds. In all cases, averaged signals were observed under titration conditions, implying that the inclusion phenomenon is a rapid and reversible process in solution. The most significant changes were those of 1,3,5-trimethoxybenzene (**II**) ($\Delta\delta = 0.41$ (*H*-Ar), 0.33 (*Me*-O)) and sodium 4-methylbenzoate (**III**) ($\Delta\delta = 0.32$ (*Me*-Ar), 0.29 ($H_{3,5}$-Ar), 0.16 ($H_{2,6}$-Ar)).

The construction of a Job plot by using the change in the chemical shift of the methoxy protons of **II** (Figure 7a) revealed a maximum at mole fraction of **II** = 0.5 with respect to the square compound, which clearly indicates 1:1 stoichiometry between the host and the square guest. When the same study was carried out monitoring the methyl ^{1}H NMR signals of **III**, a maximum at 0.67 was obtained, indicating a 1:2 stoichiometry for the host−guest association (Figure 7b). The mole ratio method provided the same results. This difference is in agreement with previous observations[87] on macrocyclic palladium systems where simple 1:1 complexation is not observed for anionic guests, possibly due to the ionic interaction on the Pd^{II} centers.

Interestingly, for the anionic guest **III** a progressive decrease was observed in the change of chemical shifts on going from the methyl group to the nearest proton to the

---

(83) Ruiz-Morales, Y.; Ziegler, T. *J. Phys. Chem. A* **1998**, *102*, 3970−3976.

(84) Schleyer, P. V.; Maerker, C.; Dransfeld, A.; Jiao, H. J.; Hommes, N. J. R. V. *J. Am. Chem. Soc.* **1996**, *118*, 6317−6318.

(85) Fujita, M.; Nagao, S.; Iida, M.; Ogata, K.; Ogura, K. *J. Am. Chem. Soc.* **1993**, *115*, 1574−1576.

(86) Fujita, M.; Ogura, K. *Coord. Chem. Rev.* **1996**, *148*, 249−264.

(87) Fujita, M.; Yazaki, J.; Ogura, K. *Tetrahedron Lett.* **1991**, *32*, 5589−5592.

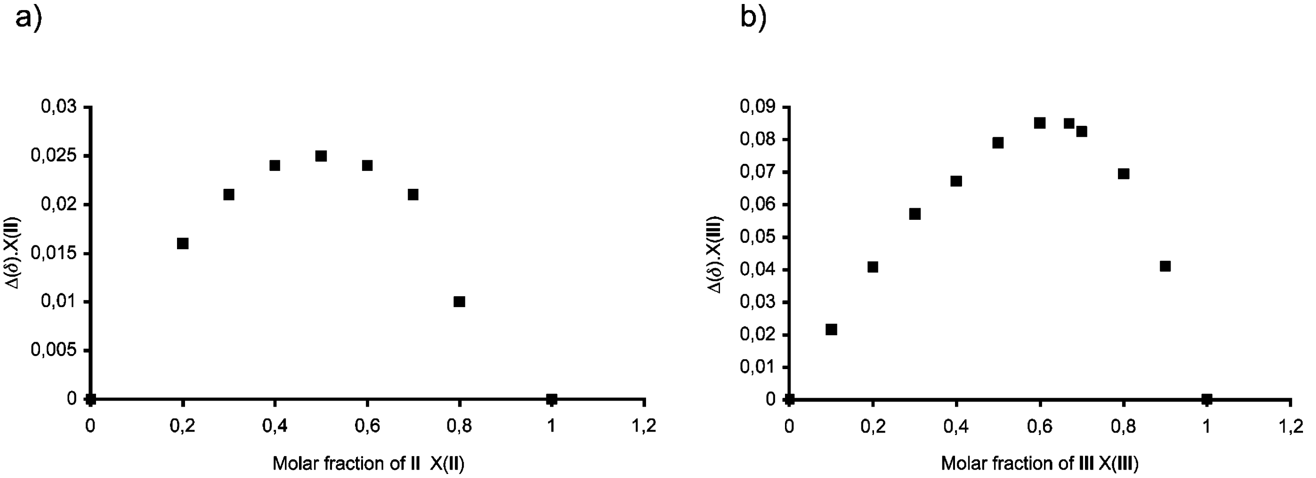

Figure 7. (a) Job plot for the binding between the palladium square **(4aA)₄** and 1,3,5-trimethoxybenzene (**II**) and (b) Job plot for the binding between **(4aA)₄** and sodium 4-methylbenzoate (**III**). The experiments were performed at 25 °C in D_2O.

carboxylate unit. As has been previously pointed out,[88] this fact could be ascribable to a form of inclusion geometry in which the hydrophobic moiety is located inside, while the hydrophilic COO^- is outside. In contrast, the symmetrical nature of **II** should not favor any particular orientation for the neutral hydrophobic guest whose protons should interact similarly with the aromatic rings of **A**.

Additionally, association constants were determined using the Chem-Equilibri program.[89,90] For the neutral guest **II**, the calculated constant $K = 38\ M^{-1}$ proved to be considerably smaller than that obtained by Fujita et al. for the analogous 4,4′-bipyridine square ($K = 750\ M^{-1}$).[87] This difference is not surprising since a weaker interaction is likely due to the larger size of **(4aA)₄** cavity (15.27 × 15.24 Å from optimized structure using the Universal Force Field) compared with Fujita's square dimensions (11.090 × 11.095 Å from the crystal structure). In the case of guest **III**, the values of $K_1 = 42$ and $K_2 = 1746\ M^{-1}$ are indicative of a cooperative effect for the binding of a second carboxylate guest. The formation of a 1:2 complex with **III** reinforces the above-mentioned idea that each of the studied guests interacts with the square host in a different way.

It is clear that the presence of the electron-deficient tetrafluorophenylene groups in **A** did not fulfill our expectations, since no increase in the host−guest interactions with respect to the 4,4′-bipyridine parent compound was observed, as shown by the low values of the corresponding calculated association parameters.

To complete these studies, it seemed interesting to investigate the extent of the interactions between the palladium square and the aromatic guests in organic media. Addition of a large excess of an aqueous saturated solution of NH_4PF_6 to a water solution of the nitrate compound **(4aA)₄** yielded a white precipitate whose NMR spectra was in accordance with the formation of the hexafluorophosphate square derivative **(4cA)₄** as a unique species (see Experimental Section). When **I** or **II** was mixed with a CH_3NO_2 solution of **(4cA)₄** ([square] = [organic compound] = 5 mM), no variation of the chemical shifts of the guests was observed. Unfortunately, however, the particular behavior of guest **III** could not be studied because of its insolubility in nitromethane. These findings confirm the importance of solvation effects on the host-binding equilibria[91] since hydrophobic neutral guests interact with hydrophobic positive charged metallomacrocyclic cavities only in aqueous media.

Conclusions

Transition metal-directed self-assembly of the fluorinated ligand 1,4-bis(4-pyridyl)tetrafluorobenzene (**A**) with 2,2′-bipyridine blocked square-planar Pd^{II} and Pt^{II} compounds resulted in the establishment of dynamic equilibria between square and triangular metallomacrocycles that have been characterized by a combination of ^1H and ^{19}F NMR spectroscopy and ESI-MS spectrometry. In striking contrast, however, when the less sterically demanding ethylenediamine was used as end-capping in the metallic corner, the formation of the square assemblies **(4aA)₄** and **(4bA)₄** as unique products has been observed. Molecular modeling studies have shown that this fact could be partially attributable to the presence of a tetrafluorophenylene ring in 1,4-bis(4-pyridyl)-tetrafluorobenzene **(A)**, since equilibrium between square and triangular entities has been detected for the nonfluorinated 1,4-bis(4-pyridyl)benzene.

While the palladium square **(4aA)₄** has been shown to be capable of acting as a host of aromatic electron-rich aromatic guests in water, its parent hexafluorophosphate derivative **(4cA)₄** did not display any spectroscopic indications of guest binding. All these experiments seem to indicate the predominance of hydrophobic over electrostatic interactions in these kinds of systems.

We are currently expanding our studies by incorporating tetrafluorophenylene units in heterometallomacrocycles of

---

(88) Fujita, M.; Nagao, S.; Ogura, K. *J. Am. Chem. Soc.* **1995**, *117*, 1649−1650.

(89) Solov'ev, V. P.; Baulin, V. E.; Strakhova, N. N.; Kazachenko, V. P.; Belsky, V. K.; Varnek, A. A.; Volkova, T. A.; Wipff, G. *J. Chem. Soc., Perkin Trans. 2* **1998**, 1489−1498.

(90) Solov'ev, V. P.; Vnuk, E. A.; Strakhova, N. N.; Raevsky, O. A. *Thermodynamic of complexation of the macrocycic polyethers with salts of alkali and alkaline-earth metals*; VINITI: Moscow, 1991.

(91) Reichardt, C. *Solvents and Solvent Effects in Organic Chemistrry*; Wiley-VCH: Weinheim, Germany, 2005.

different shapes and sizes to use them as effective receptors in molecular recognition processes.

Acknowledgment. Financial support for this work was provided by the DGICYT (Project BQU2003-01131) and the Deutsche Forschungsgemeinschaft (DFG). A.G. and M.M. thank the Universitat de Barcelona, and A.R. thanks the Studienstiftung des Deutschen Volkes for support with a scholarship. The computing resources were generously made available in the Centre de Supercomputació de Catalunya (CESCA) and the Universitat de Barcelona.

Supporting Information Available: ^{1}H NMR gCOSY, TOCSY 1D, and DOSY 2D of **$(1aA)_4$/$(1aA)_3$**, ^{1}H NMR spectra of **$(1bA)_4$/$(1bA)_3$** and **$(2cA)_4$/$(2cA)_3$**, and ESI-FT-ICR mass spectra of **$(3aA)_4$/$(3aA)_3$** and **$(3bA)_4$/$(3bA)_3$**. This material is available free of charge via the Internet at http://pubs.acs.org.

IC062373S